Coupled surface-plasmon-like modes between metamaterial

Alastair P. Hibbins,* Matthew J. Lockyear, and J. Roy Sambles
Electromagnetic Materials Research, School of Physics, University of Exeter, Exeter EX4 4QL, United Kingdom
(Received 16 July 2007; published 25 October 2007)

Perfectly conducting metals may be structured with holes to make metamaterials that support surface-plasmon-like modes at microwave frequencies. Results are presented for Fabry-Pérot-like standing wave resonances formed from coupled surface-plasmon-like modes supported by two such perforated metal substrates placed in close proximity.

DOI: 10.1103/PhysRevB.76.165431 PACS number(s): 42.25.Bs, 42.79.Dj, 73.20.Mf, 84.40.Az

The work of Ebbesen *et al.*[1] has stimulated great interest in the electromagnetic properties of subwavelength hole arrays in metal layers. The mechanism responsible for the enhanced transmission originally observed has been associated with surface plasmons (SPs).[2,3] These transverse magnetic (TM) surface waves are diffractively excited by the periodicity of the array and are tightly bound at the metal-dielectric interface, with strongly enhanced fields that decay exponentially with distance into the media either side. The SPs propagate on each face of the metal layer and their electromagnetic fields interact across the layer to induce transmission resonances whose intensities are greater than classically predicted.[4] In the visible regime, the SP decay lengths perpendicular to the interface are approximately 10^{-2} of the wavelength λ in the metal, and of the order of the wavelength in the dielectric.[5] However in the microwave (gigahertz) regime, metals almost completely screen the impinging fields (a penetration depth of approximately $10^{-4}\lambda$ into the substrate is typical), while the decay length of the fields in the dielectric extends to many hundreds of wavelengths.[6] It is therefore not surprising that microwave SPs are more commonly described as simple surface currents. Nevertheless Pendry, Martin-Moreno, and Garcia-Vidal[7] have proposed that strongly bound SP-like modes can readily be supported on the surface of suitably patterned perfect conductors; for example by forming an array of holes of subwavelength diameter. The characteristic frequency of this "metamaterial"[8] surface is the cutoff frequency ν_{cutoff} of the holes, below which only evanescent fields exist in the structured substrate. It is this exponentially decaying field property that is required for a surface mode to be supported. The aforementioned authors draw an analogy between the true surface plasma frequency of a metal, which typically lies in the ultraviolet, with this cutoff limit, the "effective plasma frequency." Importantly, the latter can be engineered by tuning the size and shape of the voids, and the dielectric properties of the material that fills them. In previous papers we discussed the excitation and propagation of these low-frequency SP-like modes on structured conducting substrates,[9] and the mode's role in enhanced transmission phenomena has also been revealed.[10] While there has been some recent debate about whether these modes should be more accurately described as "structure factor resonances,"[11] it is important to remember that the nomenclature is less important than the end result: one can strongly bind a mode to the surface of a perfect conductor by suitably texturing that surface. In other words, there exists a new tool for making metal surfaces behave in a plasmonic manner even at these low frequencies.

Here we explore the coupled surface-plasmon-like modes between two such structured conducting surfaces that together form an open-ended slit, as illustrated in Fig. 1. Went *et al.* and Yang *et al.*[12,13] have previously studied the selective transmission of microwave radiation through untextured metallic slits at microwave frequencies. Surface modes excited on opposite walls of the slit couple together across its width,[14] giving an almost plane wave in the cavity that undergoes partial reflection, due to a mode-shape mismatch, at each end. Hence a family of Fabry-Pérot (FP) standing wave resonances is established.[15] However, the familiar Fabry-Pérot equation

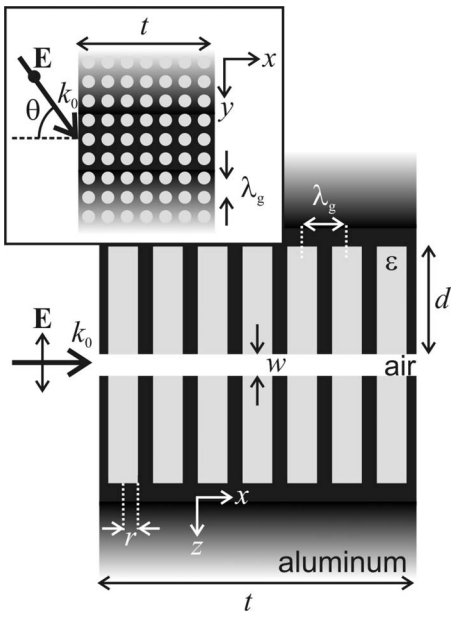

FIG. 1. Schematic illustration of the sample and experimental geometry. The plane and parallel faces of two aluminum substrates of thickness $t=30$ mm are placed a distance $w=1$ mm apart. A square array of equally spaced (λ_g), cylindrical holes (radius $r=1.57$ mm and depth $d=20$ mm) are machined into each aluminum substrate. Each hole is filled with dielectric ϵ. *p*-polarized (TM) radiation of wavelength $\lambda_0=2\pi/k_0$ is incident in the *xy* plane at an angle θ from the surface normal. The main diagram is drawn on an *xz* plane that passes through the central axis of the cylindrical holes; the inset is a top view of one of the two substrates.

$$\nu_N = c\frac{N}{2t}, \tag{1}$$

where t is the thickness of the metal substrate and N is the mode order, is exact only for this metal slit geometry in the limits of (a) infinite conductivity σ (when the coupled SP mode is entirely equivalent to a TEM waveguide mode[16]) and (b) infinitesimal slit width ($w \to 0$). ν_N represents a theoretical maximum since an increase in slit width induces end effects,[15,17] and the finite conductivity at very low slit widths results in curvature of the modes' wave fronts.[18] In the present study, the array of holes in our metal substrates induces both plasmonic and photonic behavior that strongly perturb the slit's resonant response.

The sample (Fig. 1) is formed by drilling an array of holes (radius r and pitch λ_g) into equivalent faces of two aluminum-alloy plates. The structured surfaces are then carefully aligned and spaced at their long ends with small pieces of noncompressible polyester film to yield a slit of uniform width w. The slit is orientated so that its textured faces are in the xy plane. Microwave radiation is incident in the xy plane at an angle θ from the normal to the entrance face of the slit, and is polarized with the electric field vector parallel to the z axis. A continuous wave microwave source sweeps the frequency $7.5 \leq \nu \leq 50$ GHz in bands, and feeds a fixed position horn antenna. A square aperture made from broadband microwave absorber is used to restrict the incident microwave beam to prevent leakage around the substrates. The sample is positioned on a computer-controlled rotating table to allow for automated variation in θ, and the transmitted beam is collected using a second fixed horn antenna. The data is normalized by comparison to the transmitted intensity in the absence of the sample.

In order to fully appreciate and understand our results, it is vital that we can distinguish between the effects of the photonic structure of the hole array and the more interesting surface-plasmonic-like behavior induced below the cutoff frequency of the holes. The periodic patterning of the walls on which the surface modes propagate creates bands of allowed energies separated by band gaps.[19] The lowest-energy band gap occurs at the Brillouin zone boundary at which the energy of the lower band edge is suppressed below. We optimize our structure's design, using a finite-element method (FEM) computer model (Ansoft HFSS), setting the effective plasma frequency below this lowest-energy band edge. Since the effective plasma frequency is dictated by the cutoff frequency of the holes, which for holes of infinite depth is given by[16]

$$\nu_{\text{cutoff}} = \frac{1.841c}{2\pi r\sqrt{\epsilon}}, \tag{2}$$

it is clear that this requirement can be met only by filling the holes with a high-index dielectric ($\epsilon \gg 1$). The chosen final design has seven identical holes of radius $r \approx 1.5$ mm along each metal plate of thickness $t=30$ mm (i.e., pitch $\lambda_g \approx 4.3$ mm). The metal plates are separated from one another by polyester film positioned outside the incident beam spot to provide a slit width of $w=1$ mm. Note that one expects to see a small increase in the cutoff frequency and therefore the effective plasma frequency due to the finite depth of the holes ($d=20$ mm).[10] The filling material is a mixture by weight of seven parts Dow Corning Sylgard® 170 fast cure silicone elastomer with three parts titanium dioxide (distributed by PI-KEM Ltd., grade R-1). The real part of its permittivity was determined by filling the 1 mm gaps between an array of 3-mm-wide and $t=20$-mm-thick metal slats[20] and comparing the computer predictions to the measured transmission data, which showed best agreement when $\epsilon=4.7$.

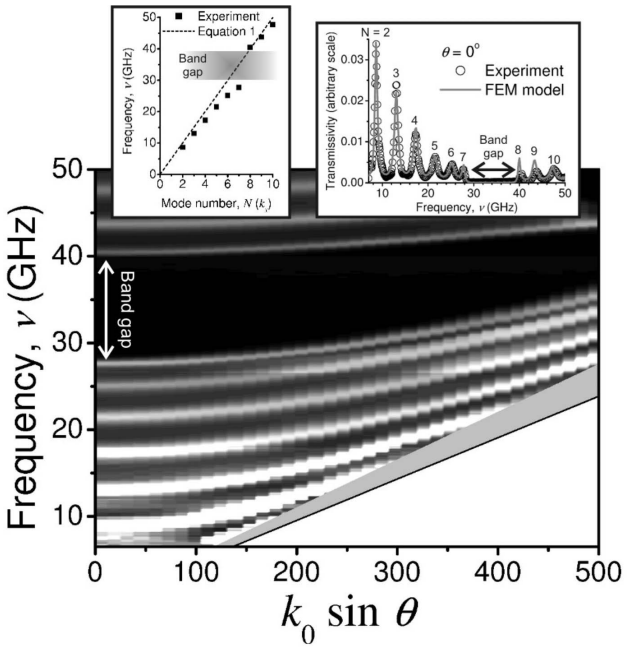

FIG. 2. Experimental transmission data recorded as a function of frequency (ν) and $k_y = k_0 \sin\theta$ from the unfilled-holes sample ($\epsilon=1$). The black solid line and the gray shaded region correspond to photons at $\theta=90°$ and angles beyond the capabilities of the experimental apparatus ($\theta > 60°$), respectively, and the band gap at $\theta=0$ is also marked. Left inset: Dispersion of $\theta=0$ modes with mode number (representative of k_x) Right inset: Comparison of experimental (circles) and modeled (line) data with radiation incident at $\theta=0$.

It is useful to first study the transmission of the sample without filling the holes. In this way, we are able to understand the origins of the photonic band structure without significant influence by any "plasmonic" perturbation since the effective plasma frequency is now beyond our frequency range of interest [$\nu_{\text{cutoff}} \approx 56$ GHz, Eq. (2)]. Figure 2 shows the experimentally measured dispersion of the FP resonances $2 \leq N \leq 10$ determined by recording transmission spectra as a function of the angle of incidence (θ). The right inset shows a $\theta=0$ line plot together with the predictions from the FEM model, where the hole radius (r) has been used as fitting parameter. The best fit to this and subsequent data is obtained with $r=1.57$ mm. While Eq. (1) predicts equally spaced FP resonances, the left inset of Fig. 2 illustrates that this equation is not valid for modes supported between our *textured* surfaces. Indeed, by plotting the resonant frequencies at $\theta=0$ as a function of mode number (N), one can determine

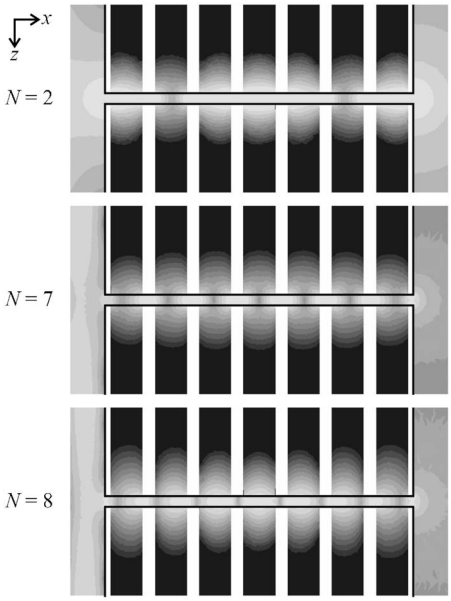

FIG. 3. FEM model predictions of time-averaged electric field magnitudes on resonance of the second, seventh, and eighth Fabry-Pérot harmonics of the air-filled hole sample. The plots represent field enhancements, using a logarithmic gray scale between 0.01 and 4, normalized to the strength of the incident field. The microwave beam is incident in the positive x direction, and the fields are plotted on an xz plane of area approximately 37×18 mm^2 passing through the central axes of the cylindrical holes. The metal regions are shaded white, and the outline of the structure is highlighted with a black line. For the seventh harmonic, the magnitude of the fields decrease exponentially into the holes with a decay length of $\sim$1.2 mm.

an approximate dispersion of the surface modes with k_x. As one would expect, the separation in frequency between FP harmonics, and therefore the group velocity of the coupled mode, reduces as the Brillouin zone boundary (between modes $N=7$ and 8) is approached. The band gap induced by the photonic surface is clearly visible. Figure 3 shows FEM model predictions of the resonant electric fields plotted on the xz plane passing through the central axes of the holes. These resonances exhibit two, seven, and eight nodes, respectively, along the slit direction. Observe also the difference in field character of the modes either side of the Brillouin zone boundary. While the resonance of the seventh harmonic exhibits electric field maxima between metallic regions of the cavity (i.e., midway between adjacent holes), the eighth harmonic exhibits maxima primarily in the regions close to the opening of the holes. It is therefore not unexpected that these standing wave solutions have very different energies.

Now consider the sample with dielectric-filled holes. The comparison between the measured and modeled data is again very good (right inset, Fig. 4), where the best fit is obtained with the imaginary part of the permittivity of the filler equal to $0.05i$. The effective plasma frequency is now ν_{cutoff} $=26$ GHz, and above this frequency one observes very little transmission because of absorption associated with waveguide resonances in the filled holes. Now, if we assume that the modes propagating on the textured surfaces inside the slit

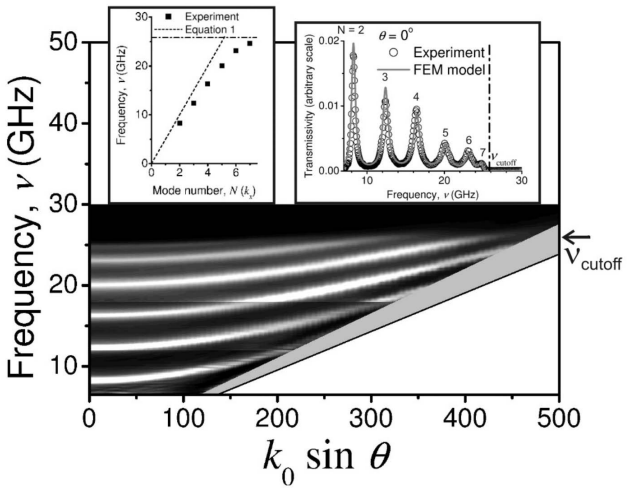

FIG. 4. Experimental transmission data recorded as a function of frequency (ν) and $k_y=k_0 \sin\theta$ from the sample with filled holes (ϵ=4.7). The cutoff frequency of the holes [Eq. (2)] is also shown. The black solid line and the gray shaded region correspond to photons at $\theta=90°$ and angles beyond the capabilities of the experimental apparatus ($\theta>60°$), respectively. Left inset: Dispersion of $\theta=0$ modes with mode number (representative of k_x). Right inset: Comparison of experimental (circles) and modeled (line) data with radiation incident at $\theta=0$.

are SP-like, we would expect the dispersion of the coupled mode to approach ν_{cutoff} with increasing values of k_x. Again we plot the resonant frequency of the FP harmonics associated with these coupled modes (left inset of Fig. 4), and the dispersion does indeed approach a limiting frequency. However, we are not able to verify the plasmonic nature of the modes based on this evidence alone, owing to the perturbation introduced by the proximity of the modes to the Brillouin zone boundary, but we can plot the dispersion of the modes with $k_y=k_0 \sin\theta$ to provide conclusive evidence. Compare the gray scale plots of Figs. 2 and 4: the modes supported by the unfilled-holes sample and also the lower band edge of the band gap show an increase in frequency approximately inversely proportional to $\cos\theta$.[21] This is the same behavior we expect to observe in the absence of surface patterning and is similar to our study since we are well below the cutoff frequency of the holes. However, for the filled-hole sample (Fig. 4) one observes a very different response. The most prominent differences are clearly apparent in the higher-order modes, and can be confidently attributed to plasmonic effects. For example, for $\theta>30°$, the frequency of the lower edge is greater than 32 GHz, compared to ν_{cutoff} $=26$ GHz. One observes an inflection point in the dispersion curves, and an asymptotic approach to the effective plasma frequency. Furthermore, notice the much longer electric field decay length into the substrate on resonance of the seventh Fabry-Pérot harmonic of the elastomer-filled hole sample (Fig. 5) compared to that of the unfilled sample at a similar frequency (Fig. 3). The magnitude of these fields decreases exponentially into the holes with decay lengths of approximately 2.8 and 1.2 mm, respectively, and is indicative of a reduction of the "effective conductivity" of these metamate-

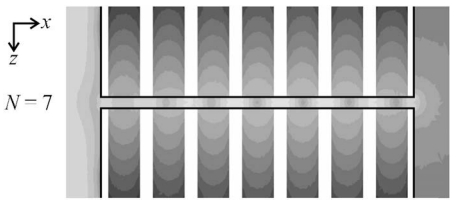

FIG. 5. FEM model predictions of time-averaged electric field magnitudes on resonance of the seventh Fabry-Pérot harmonic of the elastomer-filled hole sample. The plots represent field enhancements, using a logarithmic gray scale between 0.01 and 4, normalized to the strength of the incident field. The microwave beam is incident in the positive x direction, and the fields are plotted on an xz plane of area approximately 37×18 mm^2 passing through the central axes of the cylindrical holes. The metal regions are shaded white, and the outline of the structure is highlighted with a black line. The magnitude of the fields decreases exponentially into the holes with a decay length of ~2.8 mm.

rial surfaces that support the SP-like modes. Since it is the propagation of these modes on each surface and their subsequent coupling together that yields the Fabry-Pérot transmission resonances, a reduction in conductivity must result in a decrease in the resonant frequency for the smallest values of w due to the increased influence of the skin depth.[18] However, if skin depth is ignored, one expects the resonant frequencies of the harmonics to increase as $w \to 0$ and approach the Fabry-Pérot limit [Eq. (1)] due to the decreasing influence of end effects.[17] Therefore, for all real systems, these two competing mechanisms result in a peak value in the resonant frequency at a finite value of the slit width. For the present experiment, the resonance of the third harmonic of the filled-hole sample exhibits a maximum in the resonant frequency at a slit width of ~2000 μm (not shown). If one chooses to describe each textured substrate in the FEM model as a simple isotropic conducting medium, one can achieve a similar response by setting the metal conductivity to ~300 S m^{-1}. This should be compared to the peak in resonant frequency at ~100 μm for an untextured aluminum sample ($\sigma_{Al} \sim 10^7$ S m^{-1}).

In conclusion, we have reported the observation of coupled surface-plasmon-like modes between two closely spaced, near-perfectly-conducting substrates. While at microwave frequencies surface plasmons are better described as simple surface currents or grazing photons, subwavelength perforation of the surface induces surface-plasmonic-like behavior. For frequencies below the cutoff of the holes (i.e., below the effective surface plasma frequency), we record the dispersion of the Fabry-Pérot standing wave modes supported by an open-ended metallic slit formed from two metamaterial surfaces. Comparison of our data to the predictions of a finite-element method model confirms this mode's approach to the predicted effective plasma frequency limit. Furthermore, our model indicates an increase in penetration of the fields in the plasmonic region, indicative of a significant reduction of the "effective conductivity" of the metamaterial.

*A.P.Hibbins@exeter.ac.uk; http://www.ex.ac.uk/physics

[1] T. W. Ebbesen, H. J. Lezec, H. F. Ghaemi, T. Thio, and P. A. Wolff, Nature (London) **391**, 667 (1998).
[2] R. Sambles, Nature (London) **391**, 641 (1998).
[3] L. Martin-Moreno, F. J. Garcia-Vidal, H. J. Lezec, K. M. Pellerin, T. Thio, J. B. Pendry, and T. W. Ebbesen, Phys. Rev. Lett. **86**, 1114 (2001).
[4] H. A. Bethe, Phys. Rev. **66**, 163 (1944).
[5] H. Raether, *Surface Plasmons on Smooth and Rough Surfaces and on Gratings* (Springer-Verlag, Berlin, 1988).
[6] S. Ramo, J. R. Whinnery, and T. Van Duzer, *Fields and Waves in Communication Electronics* (John Wiley and Sons, New York, 1984).
[7] J. B. Pendry, L. Martin-Moreno, and F. J. Garcia-Vidal, Science **305**, 847 (2004).
[8] D. R. Smith, J. B. Pendry, and M. C. K. Wiltshire, Science **305**, 788 (2004).
[9] A. P. Hibbins, B. R. Evans, and J. R. Sambles, Science **308**, 670 (2005).
[10] A. P. Hibbins, M. J. Lockyear, I. R. Hooper, and J. R. Sambles, Phys. Rev. Lett. **96**, 073904 (2006).
[11] X. R. Huang, R. W. Peng, Z. Wang, F. Gao, and S. S. Jiang, Phys. Rev. A **76**, 035802 (2007).
[12] H. E. Went, A. P. Hibbins, J. R. Sambles, C. R. Lawrence, and A. P. Crick, Appl. Phys. Lett. **77**, 2789 (2000).
[13] F. Z. Yang and J. R. Sambles, Phys. Rev. Lett. **89**, 063901 (2002).
[14] S. Astilean, P. Lalanne, and M. Palamaru, Opt. Commun. **175**, 265 (2000).
[15] A. P. Hibbins, M. J. Lockyear, and J. R. Sambles, J. Appl. Phys. **99**, 124903 (2006).
[16] R. E. Collin, *Field Theory of Guided Waves* (IEEE, New York, 1991).
[17] Y. Takakura, Phys. Rev. Lett. **86**, 5601 (2001).
[18] J. R. Suckling, A. P. Hibbins, M. J. Lockyear, T. W. Preist, J. R. Sambles, and C. R. Lawrence, Phys. Rev. Lett. **92**, 147401 (2004).
[19] S. C. Kitson, W. L. Barnes, and J. R. Sambles, Phys. Rev. Lett. **77**, 2670 (1996).
[20] F. Z. Yang and J. R. Sambles, J. Phys. D **35**, 3049 (2002).
[21] When $\theta \neq 0$, k_0 and k_x are no longer collinear and there is a finite y component to the incident wave vector k_0, $k_0^2 = k_x^2 + k_y^2 + k_z^2$, where $k_y = k_0 \sin\theta$. Since $k_z = 0$ and $k_x = 2\pi/\lambda_x = 2\pi(N/2t)$ [Eq. (1)], then $k_0^2 \cos^2\theta = (2\pi)^2 (N/2t)^2$, i.e., the resonant frequency $\nu \propto (\cos\theta)^{-1}$. Note that this approximation is exact only in the limit of infinitesimal slit width when there is no phase shift at the ends of the slit (see Ref. 17).